JOURNAL OF THE ROYAL SOCIETY Interface

rsif.royalsocietypublishing.org

Research

Cite this article: Van Wassenbergh S, Aerts P. 2013 In search of the pitching momentum that enables some lizards to sustain bipedal running at constant speeds. J R Soc Interface 10: 20130241.
http://dx.doi.org/10.1098/rsif.2013.0241

Received: 15 March 2013
Accepted: 17 April 2013

Subject Areas:
biomechanics

Keywords:
agamids, sprinting, aerodynamics, biomechanics, locomotion

Author for correspondence:
Sam Van Wassenbergh
e-mail: sam.vanwassenbergh@ugent.be

Royal Society Publishing
Informing the science of the future

In search of the pitching momentum that enables some lizards to sustain bipedal running at constant speeds

Sam Van Wassenbergh[1,2] and Peter Aerts[2,3]

[1]Evolutionary Morphology of Vertebrates, Ghent University, K.L. Ledeganckstraat 35, 9000 Gent, Belgium
[2]Department of Biology, Universiteit Antwerpen, Universiteitsplein 1, 2610 Antwerp, Belgium
[3]Department of Movement and Sports Sciences, Ghent University, Watersportlaan 2, 9000 Gent, Belgium

The forelimbs of lizards are often lifted from the ground when they start sprinting. Previous research pointed out that this is a consequence of the propulsive forces from the hindlimbs. However, despite forward acceleration being hypothesized as necessary to lift the head, trunk and forelimbs, some species of agamids, teiids and basilisks sustain running in a bipedal posture at a constant speed for a relatively long time. Biomechanical modelling of steady bipedal running in the agamid *Ctenophorus cristatus* now shows that a combination of three mechanisms must be present to generate the angular impulse needed to cancel or oppose the effect of gravity. First, the trunk must be lifted significantly to displace the centre of mass more towards the hip joint. Second, the nose-up pitching moment resulting from aerodynamic forces exerted at the lizard's surface must be taken into account. Third, the vertical ground-reaction forces at the hindlimb must show a certain degree of temporal asymmetry with higher forces closer to the instant of initial foot contact. Such asymmetrical vertical ground-reaction force profiles, which differ from the classical spring-mass model of bipedal running, seem inherent to the windmilling, splayed-legged running style of lizards.

1. Introduction

During sprint running in many lizard species, a bipedal gait is often observed in which the forelimbs are lifted from the ground [1–3]. Forward dynamic modelling showed that the pitching rotation that lifts the head and trunk is probably a mechanical consequence of the lizard's forward acceleration. This rotation results from the forward-directed ground-reaction forces at the hindlimb [4]. If the centre of mass (COM) of the animal lies above the line extending the hindlimb's ground-reaction force vector, a nose-up pitching moment about the COM will be present. Once the animal has reached its top speed, however, the net propulsive impulse becomes zero, and, according to the model of Aerts *et al*. [4], so does the pitching moment that results from this propulsive impulse. After the initial acceleration that will induce bipedal gait, the model thus predicts that the lizard's forelimbs must fall back to the ground (owing to gravity) as soon as the running speed becomes constant.

However, some lizards have also been observed running bipedally *without* notable forward acceleration. The teiid lizard *Aspidoscelis sexlineata*, for example, showed sustained bipedal running with generally negligible acceleration at 1 m from the lizard's starting point on a race track [5]. Some agamid species, such as the crested dragon *Ctenophorus cristatus*, are known for their long bipedal excursions over uneven terrain [6]. The south American iguanid lizards *Liolaemus lutzae* and *Tropidurus torquatus* perform sustained bipedal running on beach or dune sand [7]. Basilisk lizards (*Basiliscus* sp.) can run across water at near-constant speed for several metres following a few strides of initial acceleration [8]. Although the mechanism of aquatic thrust and lift generation in basilisks probably differs from that of terrestrially running species [9], it appears from the above-mentioned examples that acceleration is not a prerequisite for bipedal running in several lizard species.

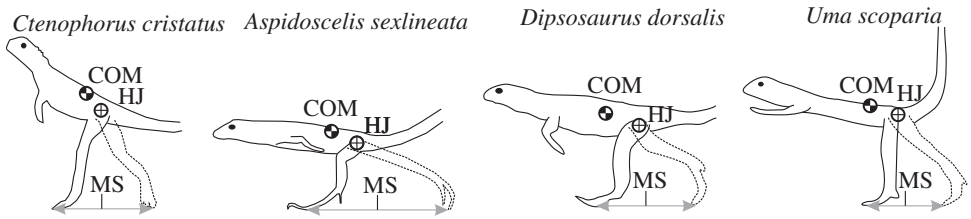

Figure 1. The running posture of four lizard species during steady bipedal running. The left hindlimb is drawn at initial foot contact, and at toe-off. The estimated relative positions of the centre of mass (COM), hip joint axis (HJ) and midstance (MS) are indicated. *Aspidoscelis sexlineata* is redrawn after Olberding *et al*. [5], and *Dipsosaurus dorsalis* and *Uma scoparia* after Irschick & Jayne [3]. The image of *Ctenophorus cristatus* is taken from high-speed video frameshots.

How bipedal running in lizards can be maintained at a constant speed is currently unknown [5]. Despite the long tail in many of these species (e.g. about 18% of body weight in *Basiliscus plumifrons*; [8]), their body COM still lies well within the anterior half of the range of footfall (footfall range defined as initial foot contact to toe-off position relative to the COM; figure 1). This implies that, over the period of foot contact, the time during which a nose-up moment is generated (upward vertical ground-reaction force vector at the foot lies in front of the downward body weight vector at the COM) will be shorter than the time in which a nose-down moment (vertical ground-reaction force vector behind the body weight vector) is generated. In order to maintain posture, however, the change in angular momentum (i.e. angular impulse) over each step (stance phase plus flight phase) must be zero. This calls for a mechanism to counteract gravity's effect of pitching the lizard nose down during steady bipedal running. The purpose of this study is to identify this mechanism.

A first option would be for the bipedal lizard to modulate the posture of the trunk and tail to displace the COM towards the hip joint. Especially when the trunk is lifted steeply, and the tail remaining horizontal, a relatively small horizontal distance between the COM and the hip joint can be expected. The more posterior the COM, the smaller the nose-down pitching effect of gravity. A similar effect could be obtained by shifting the range of footfall forward. If the medial point of this range (averaged over the stance phase) lies at the same level (or in front) of the COM, then this could directly cancel the effect of gravity. However, the few high-speed videos available of steady bipedal running in lizards do not show this effect: the midstance position of the foot is typically *behind* the COM (figure 1; [3,5,6]). Nevertheless, the relative position of the foot during stance and the position of the COM is definitely an important factor in this biomechanical problem.

A second explanation for steady bipedal running would be by means of the effect of aerodynamics. Aerodynamic forces are proportional to the square of the flow velocity [10], and bipedal lizards reach speeds as high as $4\ \mathrm{m\ s^{-1}}$ [3]. At such high speeds, the forces exerted by the air on the lizard's body surface could be a significant source of head-lifting angular impulse. However, as no information is currently available on effects of air flow on running lizards, the importance of the aerodynamic forces involved in the balance of moments about the COM remains unknown.

A third possibility is that bipedal lizards display an asymmetric profile of vertical ground-reaction forces. Imagine that the lizard would generate the entire vertical impulse to lift the body shortly following the instant of initial foot contact. In that case, the ground-reaction force vector may still be anterior of the COM, and only nose-up pitching moments would be generated. Strong asymmetry in hindlimb vertical ground-reaction force towards the instant of initial contact has been measured in quadrupedal running tegu lizards [11], but such measurements are currently not available in the literature for bipedal running in lizards. Yet, through mathematical modelling, we can explore the necessity of asymmetry in vertical ground-reaction force profiles in explaining how steady bipedal running can work in lizards.

The goal of this article is to evaluate the three above-mentioned potential sources of upper-body lifting angular momentum by means of biomechanical modelling.

2. Material and methods

2.1. Model species and CAD geometry

A renowned bipedal runner was chosen as the model species: *C. cristatus* (Agamidae). Previous work showed that more than half of this species' strides during running in a laboratory environment were bipedal [6]. The external, three-dimensional shape of the body (excluding the limbs) of an adult specimen (total length of 0.302 m) was quantified using the ellipse method [12]. To do so, by tracing the contours of the body on pictures (used with permission from herpetologist photography databases) from a lateral and dorsal view (figure 2*a*), the height and width of the body at any point along the medial axis could be determined. The ellipse method assumes elliptical shapes for each cross section, and has proved to provide accurate volume estimates of animals [12].

These elliptical cross sections were used to construct the model geometry in the CAD program Gambit v. 2.4.6 (Ansys Inc., Canonsburg, PA, USA) as a series of frustums (figure 2*b*). The front- and hindlimbs were added as elliptical cylinders, each of which width and height correspond to distances measured on the pictures. To avoid unnatural flow patterns owing to sharp edges, the elbows, knees, hands and feet were added as spheres. The limbs were rotated into a typical bipedal running position: slightly retracted upper arms, vertical lower arms and a realistic midstance position for the hindlimbs (figure 2*c*). While the head was always kept in a horizontal position to allow frontal vision, the trunk and tail were each rotated by 0°, 25°, 50° and 75° (figure 2*c*). In this way, models of 16 combinations of head and trunk angles were constructed.

For each model, the position of the centre of volume was calculated numerically: the Gambit geometry was exported as a standard ACIS text (.SAT) file, and imported into Ansys Meshing v. 14.0 to mesh it internally by more than 10^4 tetrahedra. Volumes and centroid positions of these tetrahedra were then used to calculate the centre of volume. As an approximation of the mean density of non-avian reptile bodies, the model was filled with homogeneous material of $1000\ \mathrm{kg\ m^{-3}}$ [13], and total body mass could be calculated. Owing to the assumed isotropy, all COM positions correspond to the centres of volume of the models. The effect of including lungs was tested by extruding

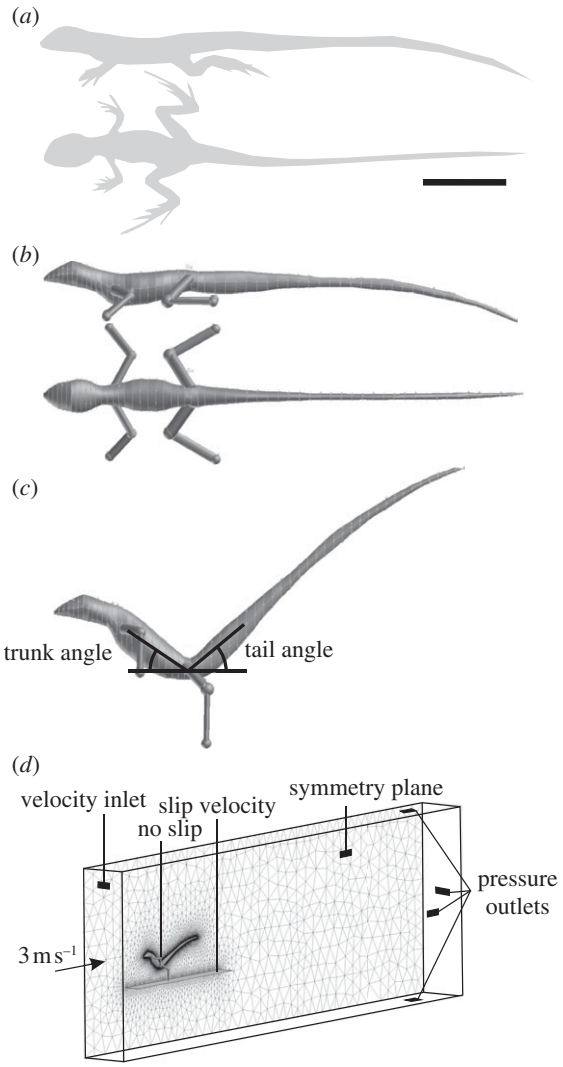

Figure 2. Steps in modelling the geometry in preparation of CFD simulations of bipedal running in *Ctenophorus cristatus*. In (*a*), contours of the body in lateral and ventral view are aligned with each other. Digitized body contours were converted into a CAD volume with elliptical cross-sectional areas (*b*). The model is rotated into a bipedal posture (*c*). The final flow domain and mesh (only shown for the midsagittal symmetry plane) with the different boundary conditions of the computational fluid dynamics model (*d*). Scale bar, 50 mm.

two lung-sized cylinders (diameter = 5 mm, length = 20 mm) from the trunk of the 50° trunk and 25° tail model. The effects owing to the calculated shift of the centre of volume (0.47 mm backward, 0.11 mm downward) and reduction in mass (0.65 g) were simulated assuming an identical shift in the centre of volume for the models with other trunk and tail postures (implying a slightly exaggerated effect for simulations with trunks inclined steeper than 50°, and slightly underestimated for more horizontal trunk orientations).

2.2. Computational fluid dynamics

To assess the magnitude of aerodynamic forces exerted at the surface of the lizard, computational fluid dynamics (CFD) simulations were performed. First, the Gambit geometry was imported into Ansys Designmodeler v. 14.0 to add other components of the airflow domain (figure 2*d*). A midsagittal symmetry plane was created to minimize computational time. A rectangular outer boundary of the domain was designed to allow sufficient space in front, behind and at the sides of the lizard. These outer boundaries include a velocity inlet in front of the lizard, and pressure outlets at the sides and back boundary (figure 2*d*). The surface of the lizard was set as a no-slip wall to include the effects of viscous shear forces by the flow. A thin plateau mimicking the ground was placed under the lizard's feet to account for aerodynamic ground effects. This ground plateau was assumed to have a slip velocity at the surface that equals the inflow velocity: ground and incoming air are thus not moving relative to each other as in a situation where the lizard runs in a wind-still environment.

A mesh of about 8.5 million tetrahedra was created for the air surrounding the lizard using Ansys Meshing v. 14.0. To promote accuracy in the most important zones, the finest mesh elements were defined at the surface of the lizard and have a triangle size of 0.2 mm (figure 2*d*). A mesh convergence test showed that only an increase of 1.2 per cent in drag force and 1.4 per cent in pitching moment about the feet was calculated, refining this mesh to a triangle size of 0.1 mm (more than 20 million cells). Given the explorative purpose of this study, we feel that a numerical error of a few percentage points is acceptable, and that this minor inaccuracy is outweighed by the advantage in computational time.

An inflow velocity (v) of 3 m s^{-1} was used, which corresponds to a speed that is reached by most medium-sized lizards during bipedal running [3,4]. To what Reynolds number (Re) this flow regime corresponds, depends on the equation

$$Re = \frac{\rho v L}{\mu}, \tag{2.1}$$

where L is the characteristic length of the object measured along the flow direction, ρ is the density of air at 20°C (1.2 kg m^{-3}) and μ is the dynamic viscosity of air at 20°C (1.82×10^{-5} Pa s). When the lizard runs in a horizontal posture, we need to consider the entire body length as L (=0.3 m) so that $Re = 59 \times 10^3$. At this Re, the wake will show turbulent flow patterns, but the boundary layer is still laminar, because it should only start a transition to turbulence from $Re = 200 \times 10^3$ [14]. This would thus only occur at running speeds higher than 10 m s^{-1}. Furthermore, the Reynolds number will even be lower for more vertical postures.

As the boundary layer is laminar at the above-mentioned Reynolds numbers, the standard laminar flow model (full Navier–Stokes equations) can be used in our CFD simulations. However, roughness of the surface may cause an earlier transition to turbulence in the boundary layer. The skin of *C. cristatus*, indeed, shows a rather rough surface because of the scales. Therefore, one simulation with a turbulence model that was specifically designed for relatively low Reynolds number flows, namely the transitional Menter shear stress transport model, was performed for a surface roughness height of 0.5 mm (an estimated average of spine height and scale groove depth in *C. cristatus*). This showed an increase in drag force and moment about the foot of about 10 per cent. Given that also the elliptical cross sections may be slightly more streamlined than the real animal, we decided to increase the aerodynamic force and moment output from the laminar flow models by 10 per cent in all further calculations to avoid underestimations by accounting for effects of surface shape imperfections.

The Reynolds-averaged equations of motion for fluid flow were solved numerically through the finite-volume method using Ansys Fluent v. 14.0. The following settings for spatial discretization were used: the pressure-based solver (chosen to obtain fast converging solutions) was used with a node-based Green–Gauss gradient treatment. According to the Ansys Fluent user manual, the latter treatment achieves higher accuracy in unstructured tetrahedral grids compared with the cell-based gradient treatment. The PRESTO! pressure discretization scheme was used for the pressure calculation and a second-order upwind scheme was used for the momentum equations. The pressure–velocity coupling was solved using the SIMPLEC scheme, which was chosen to optimize the convergence time. The latter is a discretization method that uses a relationship

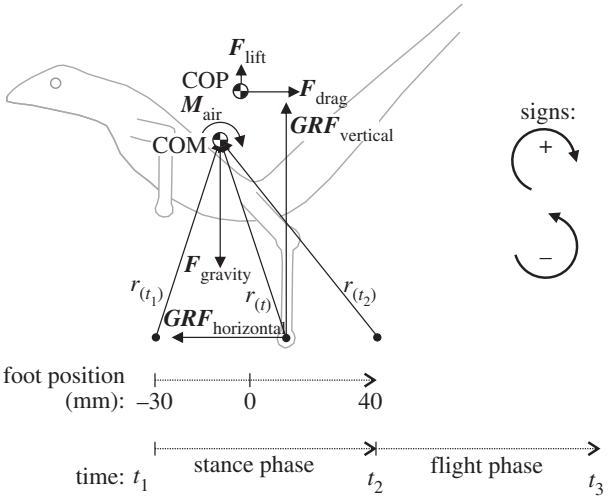

Figure 3. Forces, moments and distances involved in calculating linear and angular momentum during steady bipedal running in *Ctenophorus cristatus* (left). The sign definition used in the rest of this article for rotations, moments, angular momentum and impulse is given on the right. COP, centre of pressure.

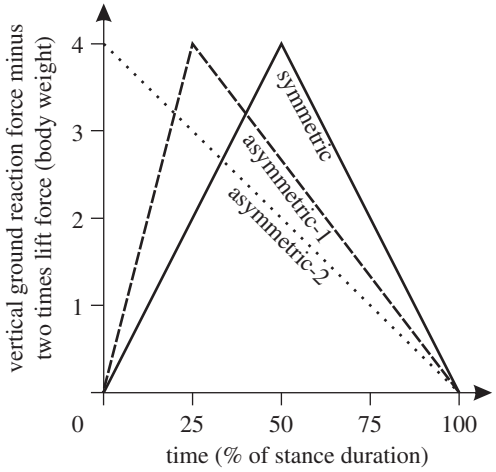

Figure 4. The three synthetic ground-reaction profiles used in the analysis: a symmetric profile, an asymmetric profile peaking at 25% of stance duration ('asymmetric-1'), and an asymmetrical profile peaking at 0% of stance duration ('asymmetric-2').

between velocity and pressure corrections to enforce mass conservation and to obtain the pressure field. Iterative convergence was reached after 1000 iterations. Total drag force, lift force and moment about a left–right axis through the COM were computed using Ansys FLUENT v. 14.0, always taking both pressure forces and viscous forces into account.

2.3. Pitch momentum–impulse calculation

The duty factor of each hindlimb (the percentage of the stride duration when a given foot is on the ground) was assumed to be 25 per cent. This is the average value reported for bipedal running in lizards [3], which also corresponds well with a lateral-view high-speed video of bipedal running of our model species *C. cristatus* (BBC, J. Brickell, used with permission). This implies that the flight phase last equally long as the stance phase. The time of foot impact on the ground was defined as t_1 (first video frame in which the toe tip penetrated the sand, and strong digit flexion was observed), toe-off takes place at t_2 (one frame prior to the release of the toe tip from the sand), and flight phase ends at t_3. The position of initial foot contact, determined as accurately as possible from the step with the best lateral view on the above-mentioned video footage, was set at 30 mm in front of the hip joint, and toe-off at 40 mm behind the hip joint (figure 3). Instantaneous foot contact was assumed to move at a constant speed from the initial contact point to the toe-off position. With a running speed of 3 m s^{-1}, this means that a stride lasts 93.4 ms (10.7 Hz stride frequency). A sensitivity analysis will be performed to evaluate how sensitive the outcome of the model is to shifts in the position of the range of footfall.

During the stance phase (t_1 to t_2), the instantaneous sum of the external forces exerted on the lizard (figure 3) in the vertical direction ($\boldsymbol{F}_{\text{vertical}}$) and horizontal direction ($\boldsymbol{F}_{\text{horizontal}}$) are, respectively,

$$\boldsymbol{F}_{\text{vertical}}(t) = \boldsymbol{GRF}_{\text{vertical}}(t) + \boldsymbol{F}_{\text{gravity}} + \boldsymbol{F}_{\text{lift}} \quad (t_1 \text{ to } t_2) \tag{2.2}$$

and

$$\boldsymbol{F}_{\text{horizontal}}(t) = \boldsymbol{GRF}_{\text{horizontal}}(t) + \boldsymbol{F}_{\text{drag}} \quad (t_1 \text{to } t_2), \tag{2.3}$$

where $\boldsymbol{GRF}_{\text{vertical}}$ and $\boldsymbol{GRF}_{\text{horizontal}}$ are the instantaneous vertical and horizontal ground-reaction forces, $\boldsymbol{F}_{\text{gravity}}$ is the gravitational force on the lizard (mass × 9.81 m s^{-2}), $\boldsymbol{F}_{\text{drag}}$ is the aerodynamic drag force and $\boldsymbol{F}_{\text{lift}}$ is the aerodynamic lift force (note that bold symbols denote vectors). Drag is defined as the total aerodynamic force in the horizontal direction opposing the running direction. Lift equals the total force in the upward vertical direction.

During the flight phase (t_2 to t_3), the external forces change to

$$\boldsymbol{F}_{\text{vertical}}(t) = \boldsymbol{F}_{\text{gravity}} + \boldsymbol{F}_{\text{lift}} \quad (t_2 \text{ to } t_3) \tag{2.4}$$

and

$$\boldsymbol{F}_{\text{horizontal}}(t) = \boldsymbol{F}_{\text{drag}} \quad (t_2 \text{ to } t_3). \tag{2.5}$$

To preserve horizontal speed and vertical position during a bipedal running bout, the vertical impulse $\boldsymbol{J}_{\text{verical}}$ and the horizontal impulse $\boldsymbol{J}_{\text{horizontal}}$ over a single step (t_1 to t_3) must be zero:

$$\boldsymbol{J}_{\text{vertical}}(t_1 \text{ to } t_3) = \int_{t1}^{t3} \boldsymbol{F}_{\text{vertical}}(t)\mathrm{d}t = 0 \tag{2.6}$$

and

$$\boldsymbol{J}_{\text{horizontal}}(t_1 \text{ to } t_3) = \int_{t1}^{t3} \boldsymbol{F}_{\text{horizontal}}(t)\mathrm{d}t = 0. \tag{2.7}$$

If we assume a constant ground-reaction force averaged throughout the stance phase, and given the equal duration of stance and flight phases, then the above conditions are fulfilled if

$$\boldsymbol{GRF}_{\text{vertical}} = -2\,\boldsymbol{F}_{\text{gravity}} - 2\,\boldsymbol{F}_{\text{lift}} \tag{2.8}$$

and

$$\boldsymbol{GRF}_{\text{horizontal}} = -2\,\boldsymbol{F}_{\text{drag}}. \tag{2.9}$$

Time-varying vertical ground-reaction profiles can be entered in the model by replacing the $-2\,\boldsymbol{F}_{\text{gravity}}$ factor in equation (2.8), as long as the time average of this new function over the stance phase still equals $-2\,\boldsymbol{F}_{\text{gravity}}$ (to obey equation (2.6)).

To evaluate the effects of asymmetry in the vertical ground-reaction force profiles, three synthetic profiles, each obeying linear momentum conservation, were used (figure 4): (i) a symmetric profile showing a linear increase to four body weights minus twice $\boldsymbol{F}_{\text{lift}}$ at midstance, followed by a linear decrease back to zero body weights at toe-off, (ii) a first asymmetric profile that shows a linear increase to four body weights minus twice $\boldsymbol{F}_{\text{lift}}$ at 25 per cent of the stance duration, again followed by a linear decrease to zero at toe-off, (iii) a second asymmetric profile that start with its maximum of four body weights minus twice $\boldsymbol{F}_{\text{lift}}$ at time 0, followed by a linear decrease to zero at toe-off. Although vertical displacements of the COM during the stance phase could theoretically have an effect on the calculated pitching moments if combined with temporal ground-reaction force asymmetry, these effects are assumed to be negligible given the relatively stable body height during running at such high step frequencies.

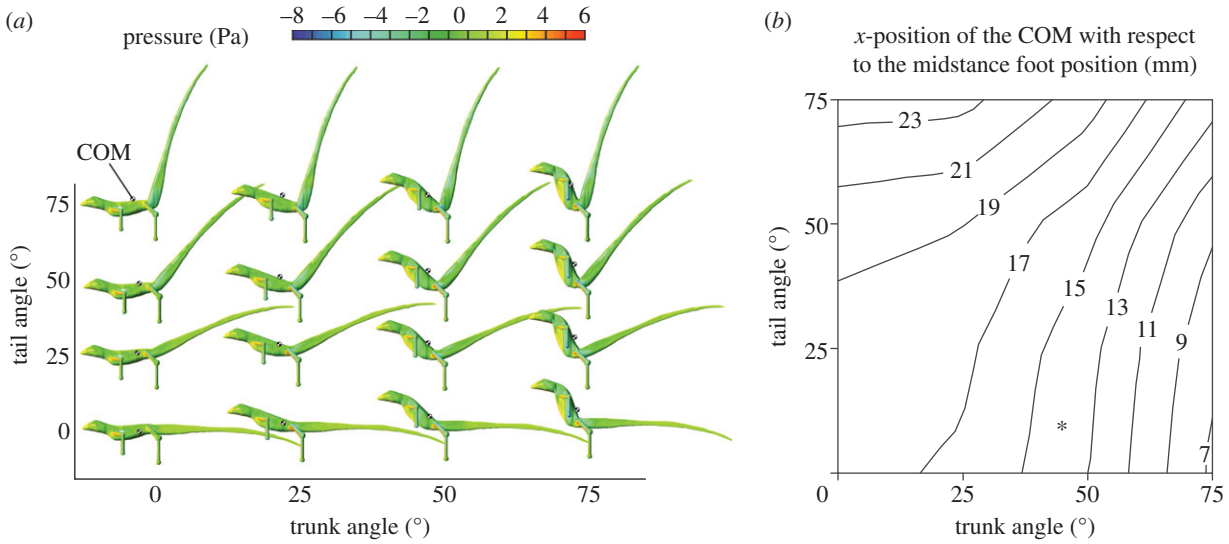

Figure 5. The effect of trunk and tail posture on the position of the centre of mass (COM). (*a*) Aerodynamic pressure on the surfaces of each of the lizard models used in the analysis (running at a 3 m s^{-1}) are shown, as calculated by computational fluid dynamics. (*b*) Isocontours of the horizontal distance of the COM in front of the midstance point of the foot (see figure 3). Asterisk denotes posture observed on video. (Online version in colour.)

The instantaneous pitching moment about the COM $\boldsymbol{M}_{\mathrm{COM}}$ is given by

$$\boldsymbol{M}_{\mathrm{COM}}(t) = \boldsymbol{r}(t) \times \boldsymbol{GRF}_{\mathrm{vertical}}(t) + \boldsymbol{r}(t) \times \boldsymbol{GRF}_{\mathrm{horizontal}}(t) + \boldsymbol{M}_{\mathrm{air}}(t_1 \,\mathrm{to}\, t_2) \tag{2.10}$$

and

$$\boldsymbol{M}_{\mathrm{COM}}(t) = \boldsymbol{M}_{\mathrm{air}} \quad (t_2 \,\mathrm{to}\, t_3), \tag{2.11}$$

where r is the instantaneous radius from the foot-contact point to the COM, and $\boldsymbol{M}_{\mathrm{air}}$ is the aerodynamic moment about the COM. The angular impulse over a single step (t_1 to t_3), $\boldsymbol{J}_{\mathrm{rotational}}$, was calculated as

$$\boldsymbol{J}_{\mathrm{rotational}}(t_1 \,\mathrm{to}\, t_3) = \int_{t1}^{t3} \boldsymbol{M}_{\mathrm{COM}}(t)\mathrm{d}t. \tag{2.12}$$

The change in angular velocity per step now equals $\boldsymbol{J}_{\mathrm{rotational}}$ divided by I_{x_COM} (the pitching moment of inertia about the COM). The impulse equations are solved numerically in Microsoft Excel by discretizing the stance phase into 100 time steps. Note that potential effects of small velocity or position changes within a single time step on the aerodynamic forces can occur, but these are probably negligible, and are therefore ignored to simplify the model.

3. Results

3.1. Effects of trunk and tail posture

The calculated horizontal COM positions varied significantly in function of tail and trunk angle in the models of *C. cristatus* (figure 5). Owing to the higher mass of the trunk and head relative to the tail, changes in the trunk angle have a larger effect. Yet, for each of the 16 trunk and tail angle configurations, the calculated COM position was anterior of the hip joint centre, and thus also anterior of the estimated midstance ground contact position 5 mm posterior of the hip joint (figure 5). This implies that the effect of gravity on the pitching balance cannot be cancelled solely by trunk and tail posture during running. The trunk and tail angle configuration of the model that best fitted the lizard's posture on the high-speed video (figure 1) were, respectively, 45° and 12°.

3.2. Effects of aerodynamics

A positive (nose up) pitching moment about the COM owing to the flow of air over the lizard can originate from three sources during steady speed running (equations (2.10) and (2.11)): (i) the direct aerodynamic moment about the COM, for example, due to higher pressure drag on the surfaces above versus below the COM, indirectly through (ii) the horizontal ground-reaction force to compensate aerodynamic drag force and (iii) the decrease in vertical ground-reaction force by aerodynamic lift.

In general, the first source (i.e. direct aerodynamic moment) only gave a positive moment for 3 m s^{-1} running when either the tail or the trunk was steeply inclined (more than 50°; maximally 7.7×10^{-5} Nm), but not together. Thus, this moment was negative (nose down) in most other cases (average = -1.7×10^{-5} Nm). Because drag force must be present, the second source always gives a positive moment, which increases with high-drag, elevated postures to 2.1×10^{-3} Nm (figure 5*a*), which in addition have a higher moment arm owing to the elevated COM position. This was the dominant source of aerodynamic moment about the COM in our lizard models. The third source, aerodynamic lift, is always present except for the horizontal trunk with tail angles of 50° or higher. The model with the highest lift was the one with the 50° trunk angle and horizontal tail angle, producing a moment of 1.3×10^{-4} Nm averaged over the step. Lift forces are only a small fraction of the body weight (maximally 1.5%) at 3 m s^{-1}.

The summed effect of all three sources resulted in a positive angular impulse about the COM per step for all model configurations. Increases in trunk angle as well as in tail angle resulted in an increased angular impulse: the change in angular velocity per step varied from 4° s^{-1} for the horizontal runner (0° trunk and tail model) to 25° s^{-1} for the 75° trunk and tail model. However, at 3 m s^{-1}, this aerodynamic impulse could not compensate the effect of gravity assuming a symmetric vertical ground-reaction profile (figure 6*a*). Assuming that aerodynamic forces scale with the square of flow velocity, we calculated that the required

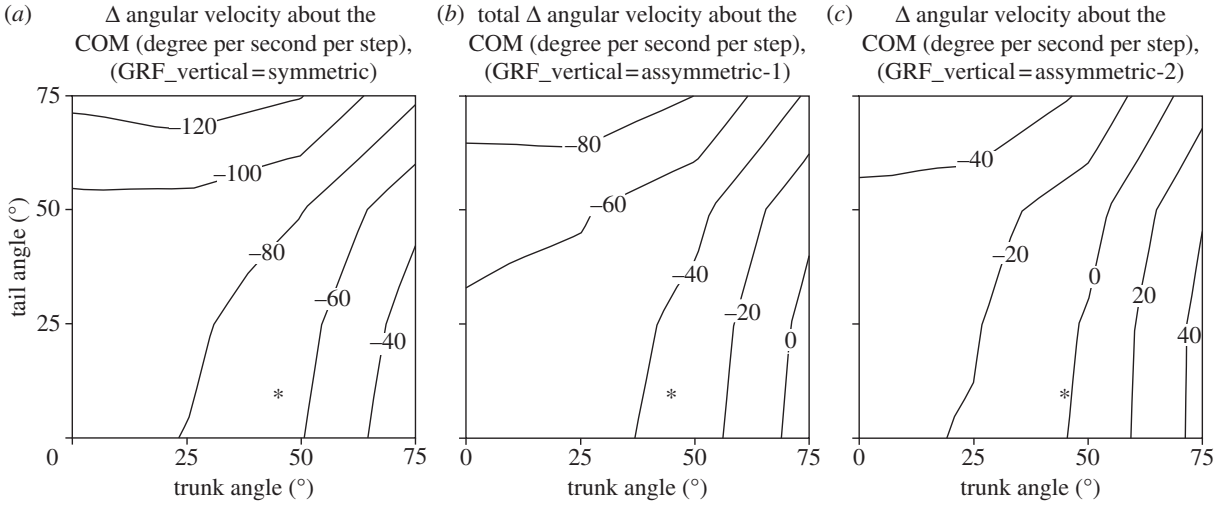

Figure 6. Isocontours of change in pitching velocity per step including all effects. Simulations were run for a vertical ground-reaction profile that was symmetrical (*a*), peaking at 25% of stance phase (*b*), and peaking at the instant of initial foot contact (*c*) as illustrated in figure 4. Asterisk denotes posture observed on video.

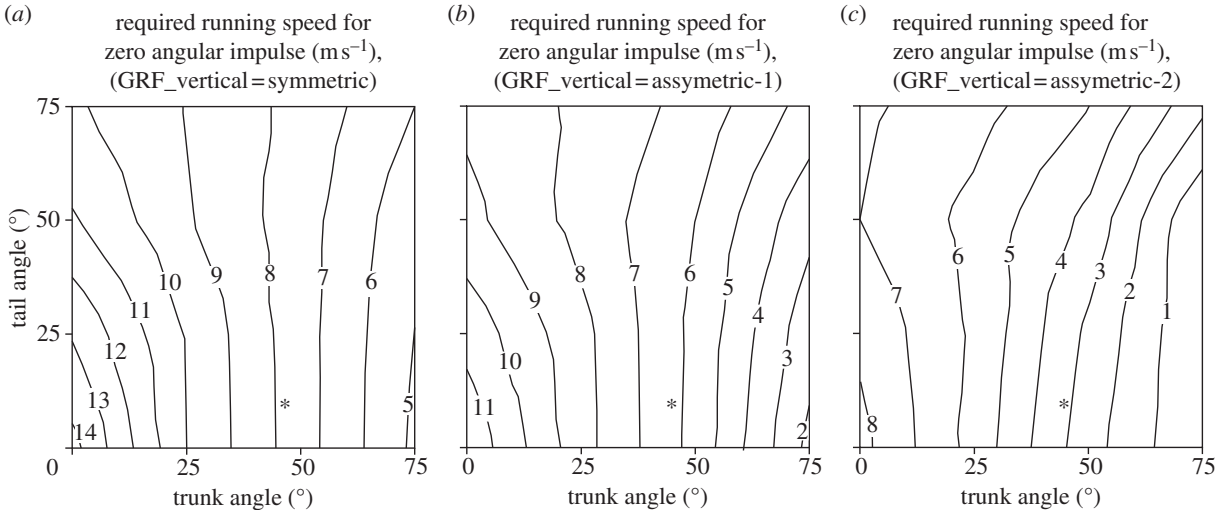

Figure 7. Isocontours of required running speed to achieve a zero pitching impulse per step. Simulations were run for a vertical ground-reaction profile that was symmetrical (*a*), peaking at 25% of stance phase (*b*), and peaking at the instant of initial foot contact (*c*) as illustrated in figure 4. Asterisk denotes posture observed on video.

running speed to achieve this compensation of the gravitational pitching moment must be significantly higher than 3 m s^{-1} (figure 7*a*): at least 5 m s^{-1} (75° trunk, 0° tail), and even 8 m s^{-1} for a 45° trunk angle (as observed on video images; figure 1).

3.3. Effects of vertical ground-reaction force asymmetry

Our model predicted that with a vertical ground-reaction force profile peaking at 25 per cent of the stance phase ('asymmetry-1' in figure 4), the model with the trunk inclined to 75° can maintain its pitching angle during steady running at realistic running speeds (between 2 and 4.5 m s^{-1} depending on the tail angle; figures 6*b* and 7*b*). The simulation with the strongest asymmetry in vertical ground-reaction force profile ('asymmetric-2' in figure 4), did achieve a zero pitching angular impulse per step approximately for the 50° trunk angle models at 3 m s^{-1} (figure 6*c*). Under the latter conditions, only steady running at trunk angles below 25° was predicted to be problematic, because the running speed then needed to be unrealistically high (more than 5.5 m s^{-1}) to achieve pitching stability (figure 7*c*).

3.4. Sensitivity to centre of mass and footfall position

The calculated posterior shift of the COM of 0.47 mm and reduction in mass of 0.6 g owing to the inclusion of two cylindrical volumes filled with air in the 50° trunk 25° tail model had a limited effect on pitching stability during steady bipedal running: the required running speed to achieve this stability reduced only by about 0.3 m s^{-1} (figure 8*a*). The forward shift in the range of footfall needed to achieve pitching stability at 3 m s^{-1} running without asymmetry in the vertical ground-reaction forces depended on the trunk and tail posture (figure 8*b*). It was minimally 6 mm anterior of the footfall range estimated on the video (figure 1) for the postures with the most posterior COM (trunk 75°, tail 0°), and increased to over 16 mm for the more horizontal postures (trunk less than 15°). The required shift was 12 mm (or 17% of the distance of the total footfall

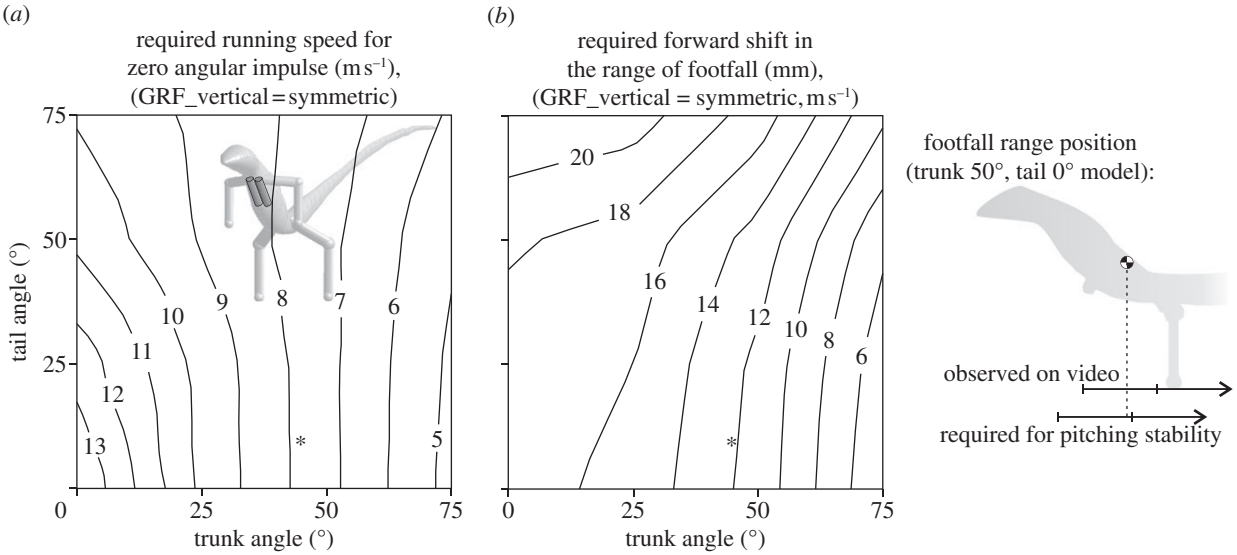

Figure 8. Results of a sensitivity analysis on the position of the centre of mass (*a*), and the footfall position (*b*). More specifically, the effect of including two cylindrical, air-filled volumes as lungs on the isocontours of required running speed (*a*), and the required forward shift in the range of footfall (*b*) to achieve a zero pitching impulse per step are shown. All models assumed a symmetric vertical ground-reaction profile, and the running speed in (*b*) was set at 3 m s^{-1}. Note that including the lungs only resulted in a negligibly small decrease in the required running speed compared with the model without lungs (figure 7*a*). At the right, the calculated shift in footfall position necessary for pitching stability during steady running (12 mm) is illustrated graphically. Asterisk denotes posture observed on video.

range) for a natural posture (i.e. trunk inclined to 45°; figure 8*b*), and 13.7 mm without aerodynamic effects when the midstance position equals the horizontal position of the COM.

4. Discussion

We described three mechanisms that can contribute to realize a stable pitching angle during bipedal running in lizards: (i) specific trunk and tail postures causing a posterior shift in the lizard's COM, (ii) aerodynamic effects and (iii) asymmetry in the vertical ground-reaction force profile. According to our model, sustained bipedal running at a constant speed in *C. cristatus* can only be achieved for a selected number of trunk and tail orientations combined with asymmetrical ground-reaction profiles.

Posture has a strong influence on the position of the COM, and hence on the pitching moment causes by gravity. Compared with a typical quadrupedal posture, the moment owing to gravity about a foot-contact point straight below the hip joint centre can reduce from −3.93 to −2.54 mN m by a 50° rotation of the trunk. The associated posterior displacement of the COM of about 5 mm is an order of magnitude higher than by including lungs in the model (figure 8*a*). Although body posture has shown to vary considerably during bipedal running [5], trunk angles of about 50° seem realistic for steady-state intervals in our model species (figure 1), and also for basilisks [8]. Note however, in this respect, that snapshots of lizards for which it was verified that they are precisely running at a constant speed are not available. Yet, even for some more extreme postures such as a trunk inclined to 75°, posture alone can never cancel the head-down moment by gravity. In addition, the average foot-contact point during a step is slightly posterior of the hip joint (figure 1), which further increases the average moment by gravity.

The flow of air around the lizard during running provides a constant source of head-lifting momentum. The magnitudes of aerodynamic pitching moments, however, are relatively low. At 3 m s^{-1}, the equivalent would be a horizontal shift in COM position of merely 2 mm (for the 50° trunk model), which is only about 30 per cent of the shift owing to posture change from a horizontal trunk to 50°. Although higher bipedal running speeds have been reported, and aerodynamic moments theoretically increase with the square of flow velocity, even a doubling of running speed to 6 m s^{-1} (higher than all reported values in the literature) does not explain how pitch angle can be maintained (figure 7*a*).

Because of the above-mentioned results for postural effects and aerodynamics, we must add a certain degree of asymmetry in the vertical ground-reaction force profile to explain steady bipedal running with our models. However, asymmetry in this profile does not correspond to the spring-mass model of bipedal running [15,16], which has proven to capture the basic pattern of mammalian bipeds [17,18]. Yet, this model was never tested for the wind-milling, splayed hindlimbs of lizards. In fact, force platform measurements of a single hindlimb during quadrupedal running in the tegu *Tupinambus merianae* did show a strongly asymmetrical profile: about 69 per cent of the total vertical impulse by the right hindlimb was generated during the first half of foot-contact time [11]. The degree of asymmetry of this measurement falls in between the two synthetic asymmetrical profiles used in our simulations (figure 4), which have 64 per cent and 75 per cent of the vertical impulse during the first half of foot-contact time. Consequently, as a hypothesis for future research measuring ground-reaction profiles of bipedal running in lizards, we also predict a relatively strong asymmetry in the vertical ground-reaction force profiles of the hindlimb during constant-speed bipedal running. Note, however, that not only the degree of asymmetry as expressed above matters, but the entire shape of the vertical ground reaction force profile relative to the COM can be important in contributing to the pitching impulse.

The mechanisms described for running on water in juvenile basilisk lizards (*B. plumifrons*) show a similar asymmetry in the push-off pattern by the hindlimb [9]. The latter study describes that the greatest vertical force (calculated from the size and intensity of the water vortices produced) was

generated during the first half of the step (the so-called slap phase), when the foot moves primarily vertically. Afterwards, when the direction of foot movement becomes predominantly backward (the so-called stroke phase), the calculated vertical forces are only one-third of the slap phase [9]. Interestingly, such a distribution of 75 per cent versus 25 per cent of the total vertical impulse over the two consecutive halves of foot-contact time is exactly what is required for our model to enable running at a stable pitching angle at 3 m s^{-1} for trunk postures with a realistic inclination of 50° (figures 6*c* and 7*c*). This could imply that the basic mechanics of bipedal running on water is not that different from running on land as might be suggested by the apparent differences in physical properties of the push-off media. In addition, it is known that loose, dry sand has material properties that can display a fluid-like behaviour [19,20]. Because bipedal running seems relatively common on this type of sandy ground [7,21,22], it would be very interesting to test whether such types of substrate promote a more asymmetrical pattern in the vertical forces by the hindlimb, and hence facilitate bipedal running.

Owing to angular momentum conservation, the windmilling rotation of the hindlimbs in the opposite sense of the nose-up pitching of the head and trunk may aid in establishing the bipedal posture. A similar rotation by the arms is intuitively performed by humans to rotate the trunk to avoid falling off the edge of a cliff. However, if we assume joint friction to be negligible, internal pitching moments are only generated to cause *accelerated* rotations of body parts. This situation does not apply to the current case of steady leg movement during constant-speed running. This means that this mechanism may help to lift the anterior body at the start of the sprint, but it cannot contribute to maintain a certain pitch angle of the body during steady running.

The most plausible advantage for lizards to sustain a bipedal gait after having accelerated to their maximal speed is their increased performance in obstacle negotiation compared with quadrupedal running [5]. During bipedal running, the inclination of the trunk increases the height of the COM, which can further be raised due to an increased hip height as a result of slightly altered hindlimb kinematics [3]. Unlike quadrupedal lizards, which must elevate the body COM prior to contacting an obstacle [23], laboratory experiments have shown that bipedal lizards perform well in maintaining a constant vertical position of the COM when overtaking an obstacle [5]. Lizards often encounter irregular surfaces with small obstacles along their travelling routes [23].

The research leading to these results has received funding from the European Community's Seventh Framework Programme (FP7/2007–2013)—Future Emerging Technologies, Embodied Intelligence, under grant agreement no. 231688. We thank M. Desclée for his work on this project, C. Clemente for providing video footage and S. Nauwelaerts for discussing this topic. We thank the three anonymous reviewers for their helpful comments and insights.

References

1. Snyder RC. 1949 Bipedal locomotion of the lizard *Basiliscus basiliscus*. *Copeia* **1949**, 129–137. (doi:10.2307/1438487)
2. Garland Jr T. 1985 Ontogenetic and individual variation in size, shape and speed in the Australian agamid lizard *Amphibolurus nuchalis*. *J. Zool. Lond.* **207**, 425–439. (doi:10.1111/j.1469-7998.1985.tb04941.x)
3. Irschick DJ, Jayne BC. 1999 Comparative three-dimensional kinematics of the hindlimb for high-speed bipedal and quadrupedal locomotion of lizards. *J. Exp. Biol.* **202**, 1047–1065.
4. Aerts P, Van Damme R, D'Août K, Vanhooydonck B. 2003 Bipedalism in lizards: whole-body modelling reveals a possible spandrel. *Phil. Trans. R. Soc. Lond. B* **358**, 1525–1533. (doi:10.1098/rstb.2003.1342)
5. Olberding JP, McBrayer LD, Higham TE. 2012 Performance and three-dimensional kinematics of bipedal lizards during obstacle negotiation. *J. Exp. Biol.* **215**, 247–255. (doi:10.1242/jeb.061135)
6. Clemente CJ, Withers PC, Thompson G, Lloyd D. 2008 Why go bipedal? Locomotion and morphology in Australian agamid lizards. *J. Exp. Biol* **211**, 2058–2065. (doi:10.1242/jeb.018044)
7. Rocha-Barbosa O, Loguercia MFC, Velloso ALR, Bonates ACC. 2008 Bipedal locomotion in *Tropidurus torquatus* (Wied, 1820) and *Liolaemus lutzae* Mertens, 1938. *Braz. J. Biol.* **68**, 649–655. (doi:10.1590/S1519-69842008000300024)
8. Hsieh ST. 2003 Three-dimensional hindlimb kinematics of water running in the plumed basilisk lizard (*Basiliscus plumifrons*). *J. Exp. Biol.* **206**, 4363–4377. (doi:10.1242/jeb.00679)
9. Hsieh ST, Lauder GV. 2004 Running on water: three-dimensional force generation by basilisk lizards. *Proc. Natl Acad. Sci. USA* **101**, 16 784–16 788. (doi:10.1073/pnas.0405736101)
10. Hoerner SF. 1965 *Fluid-dynamic drag*. Bricktown, NJ: Hoerner Fluid Dynamics.
11. Sheffield KM, Butcher MT, Shugart SK, Gander JC, Blob RW. 2011 Locomotor loading mechanics in the hindlimbs of tegu lizards (*Tupinambis merianae*): comparative and evolutionary implications. *J. Exp. Biol.* **214**, 2616–2630. (doi:10.1242/jeb.048801)
12. Drost MR, van den Boogaart JGM. 1986 A simple method for measuring the changing volume of small biological objects, illustrated by studies of suction feeding by fish larvae and of shrinkage due to histological fixation. *J. Zool. Lond.* **209**, 239–249. (doi:10.1111/j.1469-7998.1986.tb03579.x)
13. Alexander R McN. 1985 The ideal and the feasible: physical constraints on evolution. *Biol. J. Linn. Soc.* **26**, 345–358. (doi:10.1111/j.1095-8312.1985.tb02046.x)
14. Cimbala JM, Cengel Y. 2008 *Essentials of fluid mechanics: fundamentals and applications*. New York, NY: McGraw-Hill.
15. Cavagna G, Heglund N, Taylor C. 1977 Mechanical work in terrestrial locomotion: two basic mechanisms for minimizing energy expenditure. *Am. J. Physiol.* **233**, 243–261.
16. Alexander R. 1989 Optimization and gaits in the locomotion of vertebrates. *Physiol. Rev.* **69**, 1199–1227.
17. Geyer H, Seyfarth A, Blickhan R. 2006 Compliant leg behaviour explains basic dynamics of walking and running. *Proc. R. Soc. B* **273**, 2861–2867. (doi:10.1098/rspb.2006.3637)
18. Maus H-M, Lopfert SW, Gross M, Rummel J, Seyfarth A. 2010 Upright human gait did not provide a major mechanical challenge for our ancestors. *Nat. Commun.* **1**, 70. (doi:10.1038/ncomms1073)
19. Maladen RD, Ding Y, Li C, Goldman DI. 2009 Undulatory swimming in sand: subsurface locomotion of the sandfish lizard. *Science* **325**, 314–318. (doi:10.1126/science.1172490)
20. Gidmark NJ, Strother JA, Horton JM, Summers AP, Brainerd EL. 2011 Locomotory transition from water to sand and its effects on undulatory kinematics in sand lances (Ammodytidae). *J. Exp. Biol.* **214**, 657–664. (doi:10.1242/jeb.047068)
21. Summers A. 2001 Sand dune two-step: the need for speed may bring these lizards to their (hind) feet. *Nat. Hist.* **110**, 90–91.
22. Li C, Hsieh T, Goldman DI. 2012 Multi-functional foot use during running in the zebra-tailed lizard (*Callisaurus draconoides*). *J. Exp. Biol.* **215**, 3293–3308. (doi:10.1242/jeb.061937)
23. Kohlsdorf T, Biewener AA. 2006 Negotiating obstacles: running kinematics of the lizard *Sceloporus malachiticus*. *J. Zool. Lond.* **270**, 359–371. (doi:10.1111/j.1469-7998.2006.00150.x)